



Synthesis, crystal structure and biological activities of two novel organotin(IV) complexes constructed from 12-(4-methylbenzoyl)-9,10-dihydro-9,10-ethanoanthracene-11-carboxylic acid

Xiaoyan Wu^a, Wanli Kang^{a,*}, Dongsheng Zhu^{b,*}, Chaoguang Zhu^b, Shuren Liu^a

^a Enhanced Oil Recovery Research Center, China University of Petroleum, Qingdao 266555, PR China

^b Department of Chemistry, Northeast Normal University, 5268 Renmin Street, Changchun 130024, PR China

ARTICLE INFO

Article history:

Received 23 March 2009

Received in revised form 24 April 2009

Accepted 28 April 2009

Available online 7 May 2009

Keywords:

Organotin(IV) carboxylates

Synthesis

Crystal structure

Biological activity

ABSTRACT

Two complexes: $[(n\text{-Bu}_2\text{Sn})_4(\text{L})_2\text{O}_2(\text{OC}_2\text{H}_5)_2]$ (**1**) and $[(\text{C}_6\text{H}_5)_3\text{Sn}(\text{L})]$ (**2**) (where, **HL** is 12-(4-methylbenzoyl)-9,10-dihydro-9,10-ethanoanthracene-11-carboxylic acid) have been prepared and structurally characterized by means of elemental analysis and vibrational, ¹H NMR and FT-IR spectroscopies. The crystal structures of **1** and **2** have been determined by X-ray crystallography. Three distannoxane rings are present to the centrosymmetric dimeric tetraorganodistannoxane by virtue of μ_3 -oxo form the central $\text{R}_4\text{Sn}_2\text{O}_2$ core with a planar Sn_2O_2 ring, resulting in a ladder type structural motif in the molecular structure of **1**, and five-coordinated tin atoms are present in the distannoxane dimer. While the molecular of **2** adopts a monomeric distorted tetrahedral configuration with the carboxylate ligand coordinating in a monodentate mode. Both **1** and **2** exhibited good antibacterial and antitumour activities and have a potential to be used as drugs.

© 2009 Elsevier B.V. All rights reserved.

1. Introduction

The increasing interest in organotin(IV) carboxylates that has arisen in the last few decades is attributed to their significantly important biological properties like antiviral and anticancer agents, in vitro antibacterial and antifungal agents, wood preservatives and pesticides, etc. [1–11]. Several di- and tri-species have shown potential as antineoplastic and antituberculosis agents [4–7,12]. In general, triorganotin(IV) compounds display a larger array of biological activity than their di- and mono-organotin(IV) analogues. This has been attributed to their ability to bind proteins [13]. Organotin carboxylates are also of interests in view of their considerable structural diversity. Depending on the carboxylic acid used and the stoichiometry of the reactants, several products such as monomers, dimers, tetramers, oligomeric ladders, and hexameric drums can be isolated [14–18]. Steric and electronic attributes of organic substituents on tin and/or the carboxylate moiety impart significant influence on the structural characteristics in tin carboxylates. The biochemical activity of organotin compounds is also influenced greatly by the structure of the molecule and the coordination number of the tin atoms [19]. Therefore, syn-

thesis of new organotin carboxylates with different structural features will be beneficial in the development of pharmaceutical organotin and in other properties and application.

However, up to now organotin esters of 12-(4-methylbenzoyl)-9,10-dihydro-9,10-ethanoanthracene-11-acid were not reported in the literatures, to our knowledge. In order to study the structure–activity relationships of such complexes, we synthesized and characterized two novel complexes, $[(n\text{-Bu}_2\text{Sn})_4(\text{L})_2\text{O}_2(\text{OC}_2\text{H}_5)_2]$ (**1**) and $[(\text{C}_6\text{H}_5)_3\text{Sn}(\text{L})]$ (**2**) (where, **HL** is 12-(4-methylbenzoyl)-9,10-dihydro-9,10-ethanoanthracene-11-carboxylic acid). Single crystal X-ray diffraction shows that three distannoxane rings are present to the centrosymmetric dimeric tetraorganodistannoxane by virtue of μ_3 -oxo form the central $\text{R}_4\text{Sn}_2\text{O}_2$ core with a planar Sn_2O_2 ring, resulting in a ladder type structural motif in the molecular structure of complex **1**, and five-coordinated tin atoms are present in the distannoxane dimer. While the molecular of complex **2** adopts a monomeric distorted tetrahedral configuration with the carboxylate ligand coordinating in a monodentate mode. The antibacterial and antitumour activities of **1** and **2** have also been preliminary tested in vitro.

2. Experimental

2.1. General and instrumental

The reagents were used as supplied while the solvents were purified according to standard procedures [20]. Melting points

* Corresponding authors. Tel.: +86 13589332193 (W. Kang), +86 13009010567 (D. Zhu).

E-mail addresses: Kangwanli@126.com (W. Kang), zhuds206@nenu.edu.cn (D. Zhu).

were determined in open capillaries and were not corrected. Elemental analyses were carried out on a Perkin–Elmer PE 2400 CHN instrument and gravimetric analysis for Sn. ^1H NMR spectra were recorded in CDCl_3 on a Varian Mercury 300 MHz spectrometer. Infrared spectra (KBr pellets) were recorded on an Alpha Centauri FT/IR spectrometer (400–4000 cm^{-1} range). The ligand **HL** was prepared by a modified literature method [21].

2.2. X-ray crystallography

Crystals of **1** and **2** were grown by slow evaporation of ethanol solution at room temperature. The colorless crystals were mounted on a sealed tube and used for data collection. Single-crystal X-ray diffraction data for these complexes were recorded on a Bruker CCD Area Detector diffractometer by using the φ/ω scan technique with $\text{Mo K}\alpha$ radiation ($\lambda = 0.71073 \text{ \AA}$). Absorption corrections were applied by using multi-scan techniques [22]. The structures were solved by direct methods with SHELXS-97 [23] and refined by full-matrix least squares with SHELXL-97 [24] within WINGX [25]. All non-hydrogen atoms were refined with anisotropic temperature parameters, hydrogen atoms were refined as rigid groups. A summary of the crystal data, experimental details and refinement results are listed in Table 1.

2.3. Biological studies

2.3.1. Antibacterial tests

The antibacterial activities were determined by using the agar well diffusion method [26]. Broth culture medium was prepared by mixing 10 g of albumin, 3 g of beef cream, 5 g of sodium chloride and 1000 ml distilled water at 37 °C. About 5 ml of broth culture medium was poured into the petri-dishes and allowed to solidify. About 0.2 ml of broth culture medium containing approximately 10×10^6 CFU/ml of Colon or Hay bacillus was uniformly

plated on the surface of the petri-dishes prepared before. Then four wells of 3 mm diameter were made carefully and these were completely filled with the test solutions (concentration is 200 $\mu\text{g/ml}$ in ethanol), other wells containing ethanol and the reference antibacterial drug served as negative and positive controls, respectively. After the bacteria were incubated for 24 h at ca. 37 °C, the diameter of the inhibiting area around each hole was estimated, which is described as the inhibiting effect against bacteria [27]. The average of three diameters was calculated for each sample.

2.3.2. MTT assay

Hela cell lines were grown in vitro in culture media containing 10% NCS, 1% HEPES and 1% RPMI1640 in a 5% CO_2 incubator at 37 °C. The effects of di-*n*-butyltin oxide and complexes **1** and **2** on cell growth were evaluated using the MTT assay [28]. A total of 2×10^3 cells were seeded in the wells of 96-well plate and cultured for 24 h. Thereafter, the cells were treated with various concentrations (DMSO as solvent) of di-*n*-butyltin oxide and complexes for 24 h. After exposure to the drug, the MTT assay was carried out with Tetra Color One. All experiments were performed at least three times and the mean percentage of proliferation was calculated.

2.4. Synthesis

2.4.1. Synthesis of 9,10-dihydroanthracene-9,10- α,β -butanedioic anhydride

About 5.0 g (0.028 mol) anthracene, 2.75 g (0.028 mol) maleic anhydride and 52 ml xylene were added to a 100 ml three-neck boiling flask. The reaction mixture was refluxed for 2 h under stirring, then cooled to room temperature. The product crystallized under ice-water bath for 30 min, then filtrated off and washed with several milliliters of ethanol. The pure product was obtained as a white crystals. m.p. 265–266 °C, 82%.

Table 1

Crystal data and details of structure refinement parameters for complex **1** and **2**.

Complex	1	2
Empirical formula	$\text{C}_{86}\text{H}_{120}\text{O}_{10}\text{Sn}_4$	$\text{C}_{43}\text{H}_{34}\text{O}_5\text{Sn}$
Formula weight	1788.58	717.39
<i>T</i> (K)	293(2)	273(2)
Crystal size (mm)	$0.372 \times 0.352 \times 0.278$	$0.311 \times 0.279 \times 0.254$
Wavelength (Å)	0.71073	0.71073
Crystal system	Monoclinic	Triclinic
Space group	$P2(1)/n$	$P\bar{1}$
<i>Unit cell dimensions</i>		
<i>a</i> (Å)	14.4507(9)	11.502(3)
<i>b</i> (Å)	14.2478(9)	12.890(4)
<i>c</i> (Å)	20.7477(14)	13.181(4)
α (°)	90	72.899(4)
β (°)	99.3060(10)	69.611(4)
γ (°)	90	79.190(4)
<i>V</i> (Å ³)	4215.5(5)	1742.9(9)
<i>Z</i>	2	2
<i>D</i> _{calc} (g cm ⁻³)	1.409	1.367
<i>F</i> (0 0 0)	1832	732
Scan mode	ω	ω
θ Range for data collection (°)	1.60, 26.04	1.66, 26.08
Ranges of <i>h</i> , <i>k</i> , <i>l</i>	$-17 \leq h \leq 14$, $-17 \leq k \leq 17$, $-18 \leq l \leq 25$	$-14 \leq h \leq 14$, $-15 \leq k \leq 15$, $-11 \leq l \leq 16$
Reflections collected/unique	23 355/8323 [<i>R</i> _{int} = 0.0609]	9816/6708 [<i>R</i> _{int} = 0.0183]
Independent Reflections	5104	5621
Absorption coefficient (mm ⁻¹)	1.225	0.771
Final <i>R</i> indices [<i>I</i> > 2 σ (<i>I</i>)]	<i>R</i> ₁ = 0.0527, <i>wR</i> ₂ = 0.1050	<i>R</i> ₁ = 0.0382, <i>wR</i> ₂ = 0.0822
<i>R</i> indices (all data)	<i>R</i> ₁ = 0.0941, <i>wR</i> ₂ = 0.1211	<i>R</i> ₁ = 0.0492, <i>wR</i> ₂ = 0.0878
Goodness-of-fit on <i>F</i> ²	0.935	1.021
Absorption correction	Semi-empirical from equivalents	Semi-empirical from equivalents
Refinement method	Full-matrix least-squares on <i>F</i> ²	Full-matrix least-squares on <i>F</i> ²
Data/restraints/parameters	8323/6/451	6708/0/424
Largest difference peak and hole (e Å ⁻³)	0.983 and -0.660	0.636 and -0.255

2.4.2. Synthesis of HL

9,10-Dihydroanthracene-9,10- α,β -butanedioic anhydride (5.526 g, 0.02 mol), anhydrous aluminium chloride (5.334 g, 0.04 mol) and dry toluene (11.057 g, 0.12 mol) were added into a three-neck flask. The reaction mixture was stirred for 4 h at 50 °C, then poured into a beaker. After hydrolyzation with cooled aqueous HCl (20%), a brownish solid was precipitated, which collected by filtration. Then the solid was dissolved by aqueous NaOH (10%), and the surplus toluene was removed by hydrodistillation. The distilled fluid was acidified by 10% HCl, and the crude product was precipitated, then collected by filtration and washed with water. The pure product was obtained by recrystallization from ethanol as a white powder. Yield: 87.65%, m.p. 244–246 °C. Anal. Calc. for C₂₅H₂₀O₃ (368.425 g mol⁻¹): C, 81.50; H, 5.47. Found: C, 81.48; H, 5.46%. IR (KBr, cm⁻¹): $\nu(\text{O}-\text{H}\cdots\text{O})$ 3440; $\nu_{\text{as}}(\text{COO})$ 1715, 1680; $\nu_{\text{sym}}(\text{COO})$ 1460, 1415; ¹H NMR (CDCl₃, ppm): 2.34 (s, 3H, -CH₃), 3.38 (t, 1H, -CHCOOH, *J* = 4.8), 3.85 (t, 1H, -CH-COC₆H₄-, *J* = 3.2), 4.23 (d, 1H, -CH-, *J* = 5.6), 4.45 (d, 1H, -CH-, *J* = 5.2) 7.14–7.83 (m, 12H, Ar-H), 11.65 (s, 1H, -COOH).

2.4.3. Synthesis of complex [(*n*-Bu₂Sn)₄(L)₂O₂(OC₂H₅)₂] (**1**)

To a suspension of di-*n*-butyltin (0.249 g, 1 mmol) in dry benzene (30 ml) was added HL (0.368 g, 1 mmol). The mixture was heated under reflux for 8 h in a Dean–Stark apparatus for azeotropic removal of the water formed in the reaction. After cooling down to room temperature, the solution was filtered and the solvent of the filtrate was gradually removed by evaporation under vacuum until solid product was obtained. The solid was then recrystallized from ethanol to give colorless crystals of complex **1**. Yield: 58.6%, m.p. 197–198 °C. Anal. Calc. for C₈₆H₁₂₀O₁₀Sn₄ (1788.71 g mol⁻¹): C, 57.75; H, 6.76; Sn, 26.55. Found: C, 57.73; H, 6.79; Sn, 26.58%. IR (KBr, cm⁻¹): $\nu(\text{C}-\text{H})$ 2956, 2927, 2869; $\nu_{\text{as}}(\text{COO})$ 1615, $\nu_{\text{sym}}(\text{COO})$ 1385; $\nu(\text{Sn}-\text{O}-\text{Sn})$ 486, 425; $\nu(\text{Sn}-\text{C})$ 544 cm⁻¹. ¹H NMR (CDCl₃, ppm): 0.86 (t, 24H, *J* = 6.8, -CH₃); 1.1 (t, 6H, *J* = 5.7, -OCH₂CH₃); 1.32–1.38 (m, 48H, SnCH₂CH₂CH₂-); 2.38 (s, 6H, Ar-CH₃); 3.34 (t, 2H, -CH-COO-, *J* = 2.2); 3.57 (m, 4H, -O-CH₂-Me); 4.26–4.29 (t, 2H, -CH-COC₆H₄Me, *J* = 2.1); 4.52 (d, 2H, -CH-, *J* = 2.2); 4.83 (d, 2H, -CH-, *J* = 2.3); 6.9–7.9 (m, 24H, Ar-H).

2.4.4. Synthesis of complex [(C₆H₅)₃Sn(L)] (**2**)

To a suspension of Ph₃SnOH (0.367 g, 1 mmol) in dry benzene (30 ml) was added HL (0.368 g, 1 mmol). The mixture was heated under reflux for 8 h in a Dean–Stark apparatus for azeotropic removal of the water formed in the reaction. After cooling down to room temperature, the solution was filtered and the solvent of the filtrate was gradually removed by evaporation under vacuum until solid product was obtained. The solid was then recrystallized from ethanol to give colorless crystals of complex **2**. Yield: 56.8%, m.p. 118–120 °C. Anal. Calc. for C₄₃H₃₄O₃Sn (717.44 g mol⁻¹): C, 71.99; H, 4.78; Sn, 16.55. Found: C, 71.96; H, 4.81; Sn, 16.53%. IR (KBr, cm⁻¹): $\nu(\text{C}-\text{H})$ 2965, 2915, 2871; $\nu_{\text{as}}(\text{COO})$ 1665; $\nu_{\text{sym}}(\text{COO})$ 1395; $\nu(\text{Sn}-\text{C})$ 535, $\nu(\text{Sn}-\text{O})$ 235 cm⁻¹; ¹H NMR (CDCl₃, ppm): 2.41 (s, 3H, Ar-CH₃); 3.35 (t, 1H, -CH-COO-, *J* = 2.2); 4.45 (t, 1H, -CH-COC₆H₄Me, *J* = 2.1); 4.52 (d, 1H, -CH-, *J* = 2.2); 4.83 (d, 1H, -CH-, *J* = 2.3); 6.9–7.9 (m, 24H, Ar-H).

3. Result and discussion

3.1. Synthetic aspects

9,10-Dihydroanthracene-9,10- α,β -butanedioic anhydride was prepared according to Diels–Alder reaction of the anthracene and maleic anhydride. Ligand HL was synthesized according to Friedel–Crafts acylation from 9,10-dihydroanthracene-9,10- α,β -butanedioic anhydride and dry toluene in the presence of anhydrous

aluminium chloride, Scheme 1. Complexes **1** and **2** were prepared by azeotropic removal of H₂O from the reaction (in benzene) of di-*n*-butyltin oxide and triphenyltin hydroxide with HL in a molar ratio of 1:1, respectively, Scheme 2.

3.2. IR spectra

Comparing the IR spectra of the free ligand HL with complexes **1** and **2**, the bands at 3100–3550 cm⁻¹ which appear in the spectra of the free ligand as the $\nu(\text{O}-\text{H})$ vibration, are absent in those of complexes, thus indicating metal–ligand bond formation through these sites. It is generally believed that the different values in $\Delta\nu$ between asymmetric ($\nu_{\text{as}}(\text{COO})$) and symmetric ($\nu_{\text{sym}}(\text{COO})$) absorption frequencies can distinguish the ligating mode of a carboxylate moiety, that is, the value smaller than 200 cm⁻¹ indicates that the carboxylate moiety is bidentate, while the value larger than 200 cm⁻¹ indicates that the carboxylate moiety is unidentate [29,30]. The $\nu_{\text{as}}(\text{COO})$ and $\nu_{\text{sym}}(\text{COO})$ bands appear at 1615 and 1385 cm⁻¹ for complex **1** and 1665 and 1395 cm⁻¹ for complex **2**, respectively. The differences between these frequencies, $\Delta[\nu_{\text{as}}(\text{COO})-\nu_{\text{sym}}(\text{COO})]$ are close to that found for monodentate carboxylate groups (230 cm⁻¹ for **1** and 270 cm⁻¹ for **2**). This is totally consistent with the X-ray structures. The band at 486 and 425 cm⁻¹ for **1** can be assigned to the $\nu(\text{Sn}-\text{O}-\text{Sn})$ mode [31–33]. The absorption band at 544 and 535 cm⁻¹ for **1** and **2** are attribute to $\nu(\text{Sn}-\text{C})$ stretching modes, respectively [30,12].

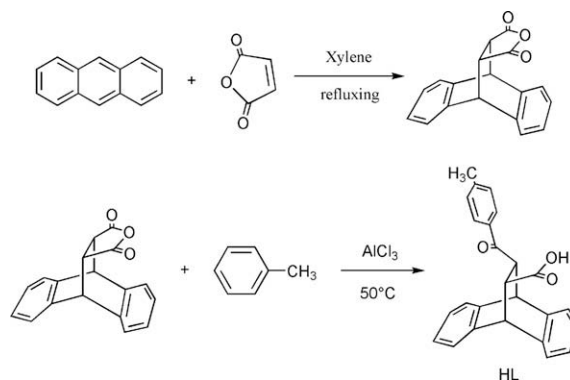
3.3. ¹H NMR spectra

The ¹H NMR spectra of the complexes **1** and **2** are given in Section 2. In the ¹H NMR spectra of ligand HL, the COOH group resonance appear at 11–12 ppm. Whereas this resonance disappear when the carboxylate group participated in coordination to the Sn atoms in complexes. The *n*-butyl protons in **1** show a multiple resonance due to -CH₂-CH₂-CH₂- skeleton in the range of 1.32–1.38 ppm and clear triple due to the terminal methyl groups at 0.86 ppm. While for **2**, the phenyl protons show a multiple in the region 6.9–7.9 ppm.

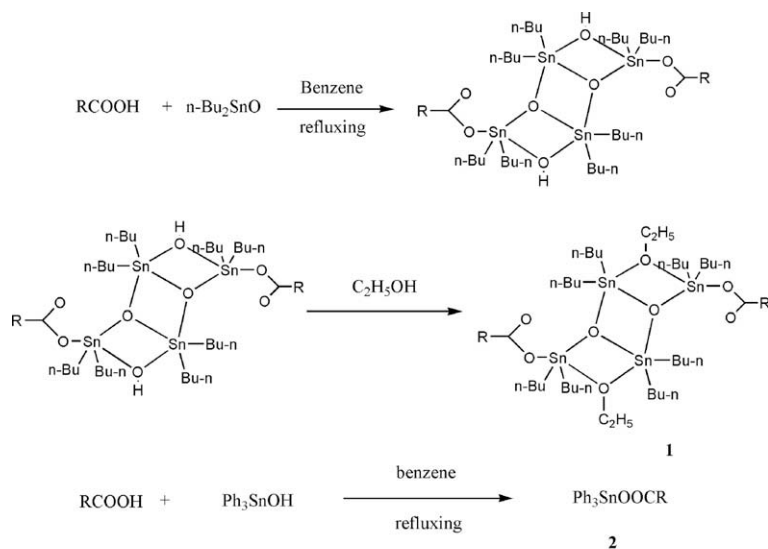
3.4. Crystal structure

3.4.1. [(*n*-Bu₂Sn)₄(L)₂O₂(OC₂H₅)₂] (**1**)

The molecular structure of complex **1** is shown in Fig. 1, selected bond distances and angles are listed in Table 2. The molecule **1** adopts a centrosymmetric dimeric structure by virtue of μ_3 -oxo [Sn(1)–O(1) 2.126(3) Å, Sn(1)–O(1A) 2.045(3) Å] which form the central R₄Sn₂O₂ core with planar Sn₂O₂ ring, resulting in a ladder type structural motif. The two oxygen atoms of this unit are tridentate as they link three Sn atoms, two *endo*-cyclic and one *exo*-cyc-



Scheme 1. The reaction scheme for synthesis of HL.



$\text{RCOOH}=\text{HL}=12\text{-}(4\text{-methylbenzoyl})\text{-}9,10\text{-dihydro-}9,10\text{-ethanoanthracene-}11\text{-carboxylic acid}$

Scheme 2. The reaction scheme for synthesis of **1** and **2**.

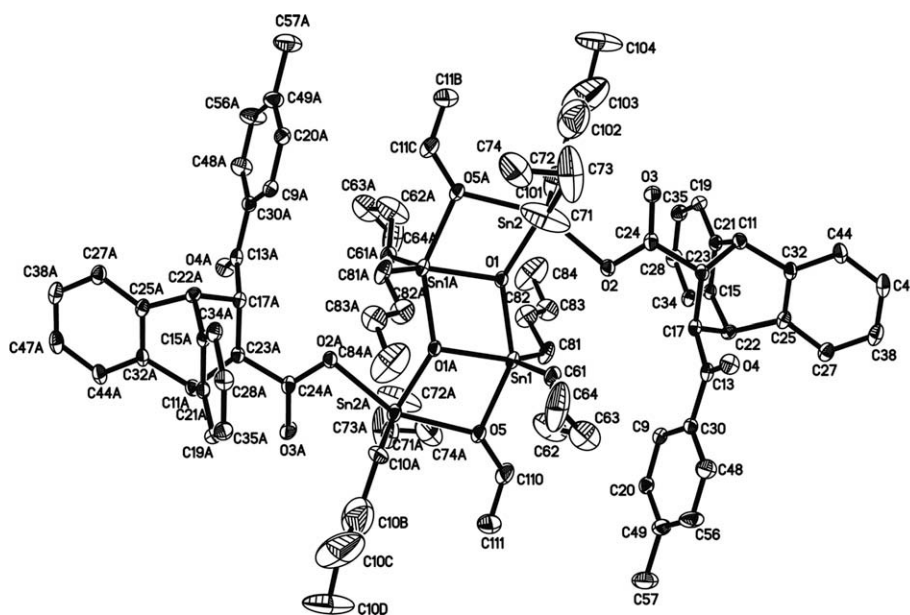


Fig. 1. Perspective view of **1** showing the atomic numbering scheme.

lic. The additional links between the *endo*- and *exo*-cyclic Sn are provided by bidentate deprotonated ethanol that form the asymmetrical bridges [Sn(1)–O(5) 2.134(4) Å and Sn(2A)–O(5) 2.263(4) Å]. Each *exo*-cyclic Sn atom is also coordinated by a monodentate carboxylato ligand (Sn(2)–O(2) 2.177(4) Å). The Sn(2)–O(3) distance 2.829 Å is considered long for primary Sn–O bonding, but represent a type of secondary interaction [34]. The bond angles are O(1A)–Sn(1)–O(1) 73.47(16)° and Sn(1A)–O(1)–Sn(1) 106.51(15)° at the μ_3 -O atom and O(1A)–Sn(1)–O(5) 74.18(14)°, Sn(1)–O(5)–Sn(2A) 100.84(15)°, Sn(2A)–O(1A)–Sn(1) 113.08(15)°, O(1A)–Sn(2A)–O(5) 71.86(14)° at the μ_2 -OC₂H₅ group.

This configuration leads to five-coordinate tin centres, each existing in a distorted trigonal bipyramidal geometry. The trigonal plane about Sn(1) is defined by the C(61), C(81) and O(1A) atoms with the axial positions being occupied by the O(1), O(5) [O(1)–Sn(1)–O(5) 147.63(14)°]. For the Sn(2) atom, the trigonal plane is

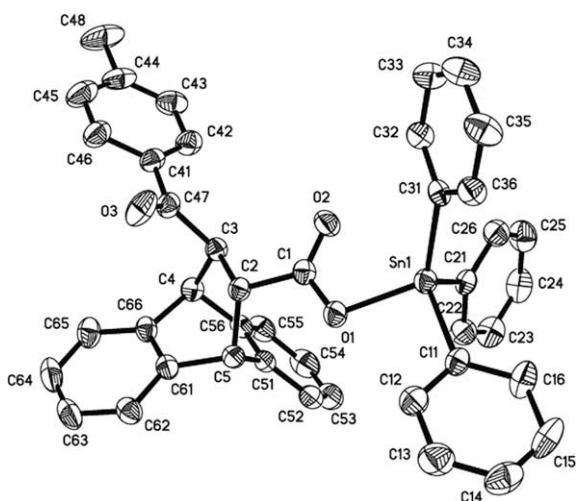
defined by the C(71), C(101) and O(1) atoms and the axial positions are occupied by the O(2) and O(5A) and the angle of O(2)–Sn(2)–O(5A) is 153.49(15)°. Distortions from the ideal geometries may be related to the close approach 2.829 Å of the O(3) atom to Sn(2). The formation of the dimeric distannoxanes **1** represents an example of ladder-type carboxylates in which the insertion of μ_2 -OC₂H₅ group occurs. Crystal structure of **1** features a μ_2 -coordination of –OC₂H₅. This result can be interpreted in terms of donor strength competition, in which the –OC₂H₅ groups show higher donor capacity than the carboxylato group of the HL [34,35].

3.4.2. [(C₆H₅)₃Sn(L)] (**2**)

The molecular structure of **2** is shown in Fig. 2, selected bond distances and angles are listed in Table 3. Complex **2** crystallizes in the triclinic space group $P\bar{1}$ with one molecule in the asymmetric unit. To a first approximation the Sn atom is four-coordinated,

Table 2
Selected bond lengths (Å) and bond angles (°) for complex **1**.

Bond lengths			
Sn(1)–O(1)#1	2.045(3)	Sn(2)–O(5)#1	2.263(4)
Sn(1)–C(81)	2.110(6)	O(1)–Sn(1)#1	2.045(3)
Sn(1)–O(1)	2.126(3)	O(2)–C(24)	1.286(7)
Sn(1)–O(5)	2.134(4)	O(4)–C(13)	1.210(6)
Sn(1)–C(61)	2.139(6)	O(3)–C(24)	1.219(7)
Sn(2)–O(1)	2.019(4)	O(5)–C(110)	1.457(8)
Sn(2)–C(71)	2.128(10)	O(5)–Sn(2)#1	2.263(4)
Sn(2)–C(101)	2.135(7)	C(17)–C(22)	1.579(7)
Sn(2)–O(2)	2.177(4)	C(11)–C(23)	1.562(8)
Bond angles			
O(1)#1–Sn(1)–C(81)	115.6(2)	O(1)–Sn(2)–O(5)#1	71.86(14)
O(1)#1–Sn(1)–O(1)	73.47(16)	C(71)–Sn(2)–O(5)#1	91.3(3)
C(81)–Sn(1)–O(1)	97.9(2)	C(101)–Sn(2)–O(5)#1	91.9(2)
O(1)#1–Sn(1)–O(5)	74.18(14)	O(2)–Sn(2)–O(5)#1	153.49(15)
C(81)–Sn(1)–O(5)	97.3(2)	Sn(2)–O(1)–Sn(1)#1	113.08(15)
O(1)–Sn(1)–O(5)	147.63(14)	Sn(2)–O(1)–Sn(1)	140.41(17)
O(1)#1–Sn(1)–C(61)	117.8(2)	Sn(1)#1–O(1)–Sn(1)	106.51(15)
C(81)–Sn(1)–C(61)	126.6(3)	Sn(1)–O(5)–Sn(2)#1	100.84(15)
O(1)–Sn(1)–C(61)	94.8(2)	O(3)–C(24)–O(2)	123.1(5)
O(5)–Sn(1)–C(61)	98.8(2)	O(3)–C(24)–C(23)	119.6(5)
O(1)–Sn(2)–C(71)	117.5(3)	C(24)–C(23)–C(17)	115.0(4)
O(1)–Sn(2)–C(101)	109.4(2)	C(13)–C(17)–C(23)	113.6(4)
C(71)–Sn(2)–C(101)	131.5(4)	C(21)–C(11)–C(23)	106.0(4)
O(1)–Sn(2)–O(2)	81.63(14)	C(32)–C(11)–C(23)	106.6(4)
C(71)–Sn(2)–O(2)	100.7(3)	C(15)–C(22)–C(17)	105.5(4)
C(101)–Sn(2)–O(2)	97.4(2)	C(24)–O(2)–Sn(2)	108.1(4)

**Fig. 2.** Perspective view of **2** showing the atomic numbering scheme.**Table 3**
Selected bond lengths (Å) and bond angles (°) for complex **2**.

Bond lengths			
Sn(1)–O(1)	2.057(2)	O(2)–C(1)	1.214(4)
Sn(1)–C(11)	2.128(3)	O(3)–C(47)	1.209(4)
Sn(1)–C(21)	2.117(3)	C(1)–C(2)	1.515(4)
Sn(1)–C(31)	2.117(3)	C(2)–C(3)	1.538(4)
O(1)–C(1)	1.305(4)	C(2)–C(5)	1.559(4)
Bond angles			
O(1)–Sn(1)–C(21)	108.05(10)	O(2)–C(1)–O(1)	120.9(3)
O(1)–Sn(1)–C(31)	117.68(10)	O(2)–C(1)–C(2)	123.6(3)
C(21)–Sn(1)–C(31)	114.12(12)	O(1)–C(1)–C(2)	115.5(3)
O(1)–Sn(1)–C(11)	93.90(10)	C(1)–C(2)–C(3)	111.9(2)
C(21)–Sn(1)–C(11)	111.68(12)	C(1)–C(2)–C(5)	112.5(2)
C(31)–Sn(1)–C(11)	109.71(12)	C(3)–C(2)–C(5)	110.1(2)
C(1)–O(1)–Sn(1)	108.40(18)		

existing in a distorted tetrahedral geometry defined by three ipso-C atoms of the phenyl groups and the O(1) atom [Sn(1)–O(1)

2.057(2) Å] of the **HL** ligand. The range of tetrahedral angles for the molecule is 93.90(10)–117.68(10)°, with the narrow and wide angles being ascribed to the influence of the non-coordinating O(2) atom. The O(2) atom approaches the tin atom at a distance of 2.735 Å, which is significantly less than 3.68 Å, the sum of their van der Waals radii for Sn and O atoms [36]. Although not considered to represent a significant bonding interaction, the influence of the O(2) atom is such that it causes the expansion of the C(31)–Sn(1)–O(1) angle [117.68(10)°] and the concomitant contraction in the O(1)–Sn(1)–C(11) angle [93.90(10)°]. Support for the conclusion that the O(2) atom does not form a significant interaction with tin is found in the disparity in the C(1)–O(1) and C(1)–O(2) bond distance of 1.305(4) and 1.214(4) Å respectively. The structure motif of complex **2** is one of the two major motif for compounds of the general formula R'CO₂SnR₃ [37].

4. Biological studies

4.1. Antibacterial activity

The antibacterial activity was performed against one Gram positive (*Bacillus subtilis*) and another Gram negative (*Escherichia coli*) bacteria, and the results are summarized in Table 4. In order to compare the results obtained, the Imipinem is used as standard drug [38]. The results indicated that both **1** and **2** show higher activity than *n*-Bu₂SnO against these two bacteria, but lower than the standard drug. The results also showed that the activity of the complexes against *E. coli* is better than against *B. subtilis*. The activity of these compounds against *E. coli* decreased in the order Imipinem > **2** > **1** > *n*-Bu₂SnO > CH₃CH₂OH and against *B. subtilis* decreased in the order Imipinem > **1** > **2** > CH₃CH₂OH > *n*-Bu₂SnO under experimental conditions. In comparison with the reported organotin carboxylates, the antibacterial activities of **1** and **2** against *E. coli* are more active than the nine organotin esters, Me₂SnL₂, Me₃SnL, *n*-Bu₂SnL₂, *n*-Bu₃SnL, Ph₃SnL, (PhCH₂)₂SnL₂, [(Me₂SnL)₂O]₂, Et₂SnL₂ and *n*-Oct₂SnL₂, where, **HL** is (E)-3-(3-fluorophenyl)-2-(4-chlorophenyl)-2-propenoic acid [39]. However, the activities of **1** and **2** against *B. subtilis* are slight less active than the nine reported compounds.

4.2. Antitumour activity

The results of cytostatic activity are summarized in Table 5. IC₅₀ values of the complexes are expressed in μM, together with that of cisplatin for comparison. Both complexes **1** and **2** showed a dose-dependent antitumour effect toward the Hela cell line. At concentrations of 10 μg/l, they provided 90% growth inhibition for **1** and 92% for **2**, and the IC₅₀ in vitro values is 1.4 and 1.2 μg/ml for **1** and **2**, respectively. Complexes **1** and **2** present lower IC₅₀ values than those of cisplatin (IC₅₀ = 3.50) [40], which indicates their high activity against the tumoral cell lines evaluated. The activity of the complexes against the Hela cell line decreased in the order **2** > **1** > *n*-Bu₂SnO. The results further demonstrated that triorganotin(IV) compounds show better antitumour activity than diorganotin(IV) compounds.

Table 4
Antibacterial screening results of **1** and **2**.

Compound	Dose (μg ml ⁻¹)	Antimicrobial circle diameter (mm)	
		G ⁻	G ⁺
CH ₃ CH ₂ OH	20	2.0	1.5
<i>n</i> -Bu ₂ SnO	20	4.6	0
1	20	15.6	9.2
2	20	18.3	9.0
Imipinem [38]	20	30	31

Concentration used: 1000 μg/ml in ethanol.

Table 5The in vitro antitumor activities of **1** and **2** against Hela cell lines.

Compound	Dose ($\mu\text{g/ml}$)	Anticancer activity (%)	IC ₅₀ ($\mu\text{g/ml}$)
<i>n</i> -Bu ₂ SnO	0.1	-5.5 ± 9.0	1.6
	0.3	18.7 ± 3.0	
	1	30.8 ± 3.2	
	3	67.0 ± 1.6	
	10	88.7 ± 0.1	
Complex 1	0.1	2.2 ± 2.8	1.4
	0.3	20.5 ± 4.4	
	1	32.8 ± 2.1	
	3	70.4 ± 0.6	
	10	90.0 ± 0.2	
Complex 2	0.1	2.3 ± 2.2	1.2
	0.3	24.1 ± 3.4	
	1	36.8 ± 5.5	
	3	72.38 ± 3.0	
	10	92.0 ± 0.2	

tin(IV) derivatives. This is well consistent with the results reported in the former literature [2,9,11,41].

In general, the antitumor activity of organotin compounds is greatly influenced by their coordination structure. The binding ability of organotin compounds towards target DNA depends on the coordination number and nature of groups bonded to the central tin atom [42]. The biocidal activity of triorganotin(IV) motifs is enhanced on account of their geometry in solution. The tetrahedral structure in solution is more active than other forms [9]. The higher activity of triphenyltin complex **2** compared to the di-*n*-butyltin **1** can be explained in terms of their coordination structures and the nature of the phenyl and *n*-butyl groups bonded to the central tin atom. In the molecule of **2**, the central tin atom is four-coordinated, existing in a distorted tetrahedral geometry, while in **1**, the tin centres are five-coordinated with a distorted trigonal bipyramidal geometry. It is also reported that the four-coordinated species has stronger tendency to increase the coordination numbers by O, S, or N donor groups while the five-coordinate species do not undergo further coordination which play no long term role in vivo chemistry of organotin(IV) esters [43–47]. Triorganotin(IV) class is more active than other classes since having a greater partition coefficient value [43,44]. As the experimental results are preliminary, further study on the antitumor effects of these compounds is highly recommended.

Acknowledgements

We acknowledged the Project (20873181) supported by the NSFC and the Project (2007AA06Z214) supported by the high-tech Research and Development Programm of China; Project is (ts20070704) supported by Taishan Scholars Construction Engineering.

Appendix A. Supplementary material

CCDC 706614 and 706814 contain the supplementary crystallographic data for complexes **1** and **2**. These data can be obtained free of charge from The Cambridge Crystallographic Data Centre via www.ccdc.cam.ac.uk/data_request/cif. Supplementary data associated with this article can be found, in the online version, at doi:10.1016/j.jorganchem.2009.04.040.

References

- [1] M. Gielen, Appl. Organomet. Chem. 16 (2002) 481.
- [2] M. Gielen, M. Biesemans, D. de Vos, R. Willem, J. Inorg. Biochem. 79 (2000) 139.
- [3] M. Gielen, M. Biesemans, R. Willem, J. Organomet. Chem. 19 (2005) 440.
- [4] M. Gielen, Coord. Chem. Rev. 15 (1996) 41.
- [5] A.J. Crowe, in: M. Gielen (Ed.), Metal-based Antitumor Drugs, vol. 1, Freund, London, 1989.
- [6] D. Kovala-Demertzi, V. Dokorou, Z. Ciunik, N. Kourkou-melis, M.A. Demertzis, Appl. Organomet. Chem. 16 (2002) 360.
- [7] V. Dokorou, D. Kovala-Demertzi, J.P. Jasinski, A. Galani, M.A. Demertzis, Helv. Chim. Acta 87 (2004) 1940.
- [8] M. Ashfaq, J. Organomet. Chem. 691 (2006) 1803.
- [9] M. Ashfaq, M.I. Khan, M.K. Baloch, A. Malik, J. Organomet. Chem. 689 (2004) 238.
- [10] M.I. Khan, M.K. Baloch, M. Ashfaq, J. Organomet. Chem. 689 (2004) 3370.
- [11] M.I. Khan, M.K. Baloch, M. Ashfaq, G. Stoter, J. Organomet. Chem. 691 (2006) 2254.
- [12] D. Kovala-Demertzi, V.N. Dokorou, J.P. Jasinski, A. Opolski, J. Wiecek, M. Zervou, M.A. Demertzis, J. Organomet. Chem. 690 (2005) 1800.
- [13] T.S. Basu Baul, C. Masharing, S. Basu, E. Rivarola, M. Holčapek, R. Jirásko, A. Lyčka, D. de Vos, A. Linden, J. Organomet. Chem. 691 (2006) 952.
- [14] R.R. Holmes, Acc. Chem. Res. 22 (1989) 190.
- [15] E.R.T. Tiekink, Appl. Organomet. Chem. 5 (1991) 1.
- [16] E.R.T. Tiekink, Trends Organomet. Chem. 1 (1994) 71.
- [17] V. Chandrasekhar, S. Nagendran, V. Baskar, Coord. Chem. Rev. 235 (2002) 1.
- [18] G. Prabusankar, R. Murugavel, Organometallics 23 (2004) 5644.
- [19] R. Zhang, J. Sun, C. Ma, J. Organomet. Chem. 690 (2005) 4366.
- [20] D.D. Perrin, W.L.F. Armarego, D.R. Perrin, Purification of Laboratory Chemicals, second ed., Pergamon, Oxford, 1980.
- [21] Charles D. Hurd, Albert Tockman, J. Am. Chem. Soc. 81 (1959) 116.
- [22] G.M. Sheldrick, SADABS, Program for Empirical Absorption Correction of Area Detector Data, University of Göttingen, Germany, 1996.
- [23] G.M. Sheldrick, SHELXS-97, A Program for Automatic Solution of Crystal Structure, University of Göttingen, Germany, 1997.
- [24] G.M. Sheldrick, SHELXL-97, A Program for Crystal Structure Refinement, University of Göttingen, Germany, 1997.
- [25] L.J. Farrugia, WINGX, A Windows-based Program for Crystal Structure Analysis, University of Glasgow, Glasgow, UK, 1988.
- [26] A. Rahman, M.I. Choudhary, W.J. Thomsen, Bioassay Techniques for Drug Development, Harwood Academic Publishers, The Netherlands, 2001. p. 16.
- [27] Z.L. You, H.L. Zhu, Z. Anorg. Allg. Chem. 630 (2004) 2754.
- [28] A. Varvaresou, K. Iakovou, Anticancer Res. 25 (2005) 2253.
- [29] B.Y.K. Ho, J.J. Zuckerman, Inorg. Chem. 12 (1973) 1552.
- [30] K. Nakamoto, Infrared and Raman Spectra of Inorganic and Coordination Compounds [M], fourth ed., Wiley, New York, 1980.
- [31] J.A. Zubita, J.J. Zuckerman, Inorg. Chem. 24 (1987) 251.
- [32] G.K. Sandhu, R. Gupta, S.S. Sandhu, R.V. Parish, Polyhedron 4 (1985) 81.
- [33] G.K. Sandhu, R. Gupta, S.S. Sandhu, R.V. Parish, K. Brown, J. Organomet. Chem. 279 (1985) 373.
- [34] V. Dokorou, M.A. Demertzis, J.P. Jasinski, D. Kovala-Demertzi, J. Organomet. Chem. 689 (2004) 317.
- [35] D. Kovala-Demertzi, V. Dokorou, R. Kruszynski, J. Wiecek, T.J. Bartczak, M.A. Demertzis, Z. Anorg. Allg. Chem. 631 (2005) 2481.
- [36] A. Bondi, J. Phys. Chem. 441 (1964) 441.
- [37] R. Willem, A. Bouhdid, B. Mahieu, J. Organomet. Chem. 531 (1997) 151.
- [38] W. Rehman, M.K. Baloch, A. Badshah, S. Ali, Spectrochim. Acta, Part A 65 (2006) 689.
- [39] Sadiq-ur-Rehman, K. Shahid, S. Ali, M.H. Bhatti, M. Parvez, J. Organomet. Chem. 690 (2005) 1396.
- [40] G.N. Kaluderović, V.M. Đinović, Z.D. Jurančić, T.P. Stanojković, T.J. Sabo, J. Inorg. Biochem. 99 (2005) 488.
- [41] S. Gómez-Ruiz, G.N. Kaluderović, S. Prashar, E. Hey-Hawkins, A. Erić, Ž. Žižak, Z.D. Jurančić, J. Inorg. Biochem. 102 (2008) 2087.
- [42] Y. Li, Y. Li, X. Niu, L. Jie, X. Shang, J. Guo, Q. Li, J. Inorg. Biochem. 102 (2008) 1731.
- [43] K.C. Molloy, in: Fr. Hartley (Ed.), Bioorganotin Compounds in the Chemistry of Metal Carbon Bond, vol. 5, Wiley, New York, 1989 (Chapter 11).
- [44] J.M. Hook, B.M. Linahan, R.L. Taylor, E.R.T. Tiekink, L. Van Gorkom, L.K. Webster, Main Group Met. Chem. 17 (1994) 293.
- [45] M. Danish, G. Alt Helmut, A. Badshah, S. Ali, M. Mazhar, Nazar-ul-Islam, J. Organomet. Chem. 486 (1995) 51.
- [46] M. Gielen, A.E.L. Khloufi, M. Biesemans, M. Mahieu, R. Willem, Bull. Soc. Chim. Belg. 101 (1992) 243.
- [47] R. Willem, H. Dalil, M. Biesemans, J.C. Martins, M. Gielen, Appl. Organomet. Chem. 13 (1999) 605.